DUJASE Vol. 3(2) 181-187, 2016 (January)

Construction and experimental study of a novel solar concentrating thermal collector

Shams S M N[1], McKeever M[2], Mc Cormack S[3] and Norton B[4]

[1]*Institute of Energy, Dhaka University, Dhaka, Bangladesh*

[2]*Dublin Energy Lab, School of Electrical and Electronic Engineering, Dublin Institute of Technology, Ireland*

[3]*Dublin Energy Lab, Department of Civil, Structural and Environmental Engineering, Trinity College, Ireland*

[4]*Dublin Energy Lab, Dublin Institute of Technology, Dublin, Ireland*

E-mail: nasifshams@gmail.com

Received on 21.12.2015. Accepted for publication on 19.01.2016.

ABSTRACT

This paper presents the thermal efficiency and thermal performance of a newly designed and fabricated Concentrating Transpired Air Heating (CTAH) system, designed solar air heating collector comprised of an inverted perforated absorber and an asymmetric compound parabolic concentrator was applied to increase the intensity of solar radiation incident on the perforated absorber.Experimental thermal efficiency remained high at higher air flow rates. The average thermal efficiency was found to be approximately 55%-65% with average radiation above 400 W/m^2 for flow rates in the range of 0.03 kg/s/m^2 to 0.09 kg/s/m^2. Experimental results at air flow rates of 0.03 kg/s/m^2 and 0.09 kg/s/m^2 showed temperature rise of 38^{o}C and 19.6^{o}C respectively at a solar radiation intensity of 1,000 W/m^2.The black colour carbon fibre plain weave with inherent lower pitch and perforation diameter combination (porosity < 5%) was adopted in the CTAH design.Highly reflective reflector material (dimension 1250mm x 1000mm x 0.5mm) was used (95% total light reflection) from the company 'Alanod'.The glazing material of the CTAH system is one 6 mm thick low iron glass cover.The air chamber was protected and insulated with thermawrap insulation from the inside and outside walls.A comparative performance study shows the thermal performance of CTAH at different flow rate. As the absorber of the CTAH facing downward, it avoids radiation loss and the perforated absorber with tertiary concentrator reduces thermal losses from the system.

Keywords: Concentrating Transpired Air Heating (CTAH), Asymmetric Compound Parabolic Concentrator (ACPC), Air Heating.

1. Introduction

Solar Air Heating Collectors (SAHC) are well established with applications in space heating and space ventilation, timber seasoning, curing of industrial products and drying [1-2].Conventional solar air heating systems inherit poor convective heat transfer coefficients between the absorber plate and the air flow which results in the absorber temperature being much higher than the air stream temperature. This causes greater heat losses to the surroundings. The heavy metallic absorber also makes air heating systems difficult to integrate in buildings[3-4].

At present, two main types of SAHC exist commercially: Unglazed Solar Air Heating Collector (USAHC) and Glazed Solar Air Heating Collector (GSAHC). The basic difference between two main types of solar air heating collectors is presence of glazing cover and design of absorber surface. UTC (Unglazed Transpired Collector) collectors do not have glazing cover and contains perforated absorber. UTC has been subject to a number of investigations [5-6]. Continuous improvements to the UTC have focused on the material of the transpired absorber [5], diameter and pitch of the perforation and thickness of the absorber [6]. However, the temperature rise of the air in UTC is comparatively much lower than that for glazed solar collectors. In order to enhance the thermal efficiency of GSAHC, different modifications were suggested and applied to improve the heat transfer between absorber and air [7-8].

An absorber placed horizontally, facing downward was presented in a previous study [9] which showed a lower radiation loss compare to the absorber surface facing the sky. A concentrating system employing inverted flat plate absorbers was demonstrated [10]in which radiation was reflected from below onto the downward facing absorber. Kothdiwala et al. (1995)[11] conducted optical parametric analysis on asymmetric line-axis inverted ACPC.This is mostly due to convection suppression at the absorber due to the formation of a pocket of hot air at tertiary section [11-13]. The usefulness of the CPC for solar energy collection was noted by numerous researchers [14-15]. Several researchers[16-18]suggested that the concentrator design should be highly asymmetric at high latitude. The ACPC is a transformed form of a non-imaging CPC. Truncation of the reflectors of an ACPC reduces the size and cost of a system but results in a loss of concentration [17].

Comparatively little experimental research has been carried out [19-20]to improve solar air heating system performance using concentrators. Pramuang&Exell (2005) [20] modelled concentrator integrated non-perforated absorber water heating collector. Tchinda (2008) [19] modelled concentrator integrated non-perforated absorber air heating collector. Numerous researches have been carried out on PV integrated solar air heating systems [22-23].However, integration of inverted perforated absorber with ACPC concentrator for air heating purpose has not been

investigated.In order to overcome the limitations inherent with conventional solar air heating systems, a new type of air heating system has been proposed in this research.

2. Construction of the concentrator system

Schematic diagram of the CTAH system is presented in Figure 1.which is a combination of transpired absorber, Asymmetric Compound Parabolic Concentrator (ACPC), tertiary reflector and glazing cover. The vital components of CTAH are as below:

1) Inverted perforated absorber: A perforated absorber has been incorporated in the design which faces downward to reduce radiation loss. Perforated surface allows air to flow through the absorber which enhances heat transfer between the absorber and flowing air. Solar air heaters are generally constructed using metal plates as the absorber of the incident solar radiation which introduces conduction losses. The concentrator of the system works as an amplifier which increases the amount of solar radiation on a decreased absorber area.

2) Concentrator: A concentrator has been introduced with the perforated absorber for the first time to increase the concentration of the incident solar radiation onto the inverted perforated absorber. ACPC in CTAH has been designed with upper and lower reflectors of identical reflectance. The secondary circular part of the concentrator in CTAH concentrates all incident radiation on the inverted absorber. The concentration ratio between inlet and outlet of the secondary circular reflector is 1.Concentration of solar radiation becomes necessary when higher temperatures are desired. Heat losses from the collector are proportional to the absorber area. Concentration ratio is the ratio of aperture area to absorber area. So, heat losses are inversely proportional to the concentration.

3) Tertiary reflector section: A parallel reflector section just below the inverted absorber helps to improve the stratified thermal layer below the absorber which enhances the heat transfer mechanism.

4) Glazing cover: A glazing cover has been introduced which works as the heat trap for the emitted radiation from the absorber surface. However, an optical loss occurs due to the reflection and absorption on the glazing cover. A high transmittance glazing material reduces the optical loss. Also during outdoor operation a glazing surface is necessary to provide protection from dust deposition, rain and wind. In conventional solar collectors a parallel glazing cover usually orients with absorber surface to reduce the reflection loss. However the design introduces convection loss from the glazing cover and radiation loss from the absorber surface. Air inlet is located at the side wall of the CTAH.

Figure 1 shows Schematic Diagram of the CTAH.

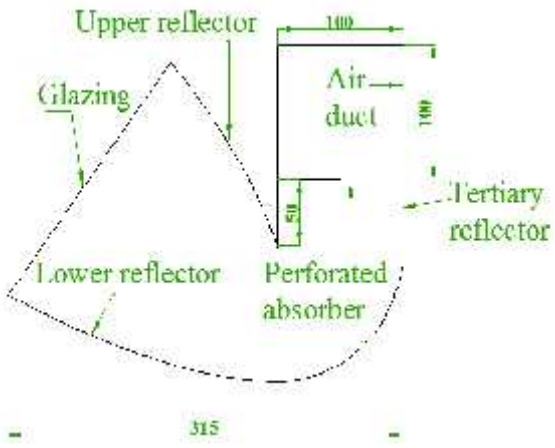

Fig. 1: Schematic Diagram of the CTAH

3. Experimental Analysis

3.1 Experimental setup:

The experimental setup used in experimental study consisted of a standard outdoor test facility fully instrumented for air collector testing. Wind speed, ambient temperature, input air temperature, output air temperature, ambient temperature, absorber surface temperature, tertiary cavity air temperature, air flow rate, glazing surface temperature, solar radiation on the surface of the aperture and on horizontal surface were measured. The experiments were carried out for the close loop CTAH system. A schematic diagram of the closed loop experimental system CTAH has been shown in Figure 2. The inlet of the CTAH collector was connected with the air duct. The outlet of the CTAH collector was connected with a fan unit. The fan unit extracted air from the collector and supplied it to the air chamber. The air chamber and CTAH collector were connected with the air duct.

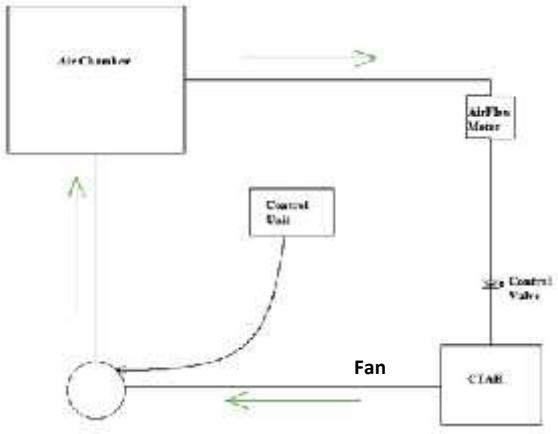

Fig. 2: Closed loop outdoor experimental setup of CTAH

Air flowed through the air duct to the collector. The integrated flow meter in the air duct measured the air flow rate. Figure 3 shows the CTAH with air inlet duct. Figure 4 shows the outdoor experimental setup with air chamber and

the air fan unit.A waterproof plastic cover was used to protect the CTAH collector. The air flow meter was integrated with the air inlet duct. The input of the inlet duct and air chamber was connected with a flexible air duct. The air chamber was protected and insulated with thermawrap insulation from the inside and outside walls. The fan was enclosed and protected from the environment during outdoor experiments.

3.2 Experimental results at zero air flow

The instantaneous stagnation absorber temperature reached 135.9°C on 17th of August as shown in Figure 5. The absorber temperature and ambient temperature for CTAH are shown in Figure 5 for zero air flow rate (stagnation condition) on 17th August, 2011.

Fig. 3: Outdoor experimental setup with CTAH and long inlet duct

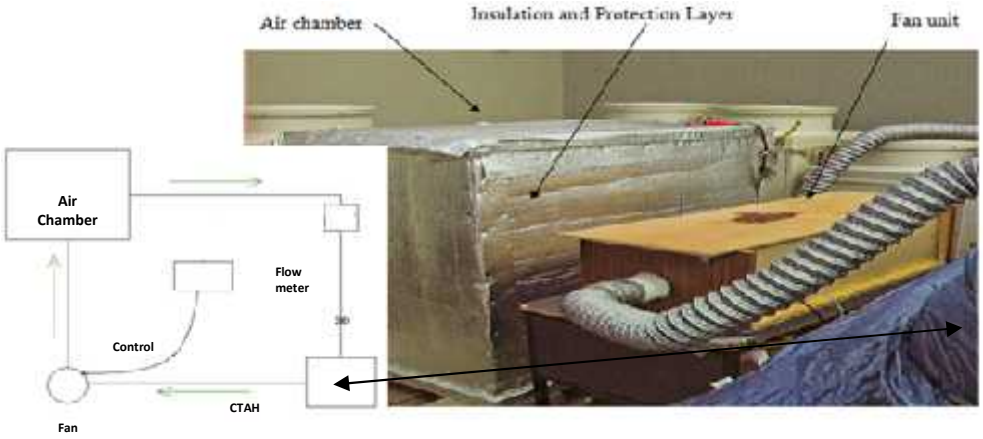

Fig. 4: Outdoor experimental setup with the air chamber and fan unit

The experiments were carried out for the close loop CTAH system.The technical specifications of experimental prototype are shown in Table 1.

Table 1: Technical specifications of the experimental prototype

Absorber material	Absorber porosity (%)	System type	Tertiary height (mm)	Air flow
				Low ($kg/s/m^2$)
Carbon fibre	4.2	Closed loop	50	0.03

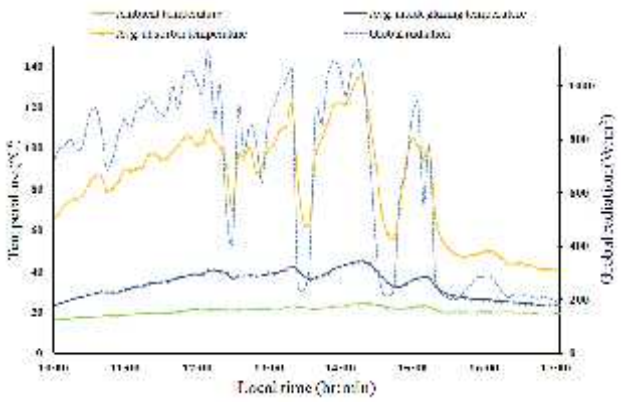

Figure 5: Absorber and ambient air temperatures of the CTAH*for prototype* at zero flow *rate*

The entrance and exit of the CTAH were closed to conduct the stagnation experiment. The temperature of the glazing, air near glazing, air in tertiary cavity and the absorber surface were measured. The temperatures were measured over the day to investigate the effect of solar radiation variation over time.The experimental results also indicated the maximum absorber temperature without air flow. The maximum glazing surface temperature was 45.3^{o}C. The difference in temperature between the absorber and ambient air was 115^{o}C. Most of the local sunny days were with intermittent cloud cover. Figure 6 shows the hourly stagnation performance of the CTAH on 17th August.

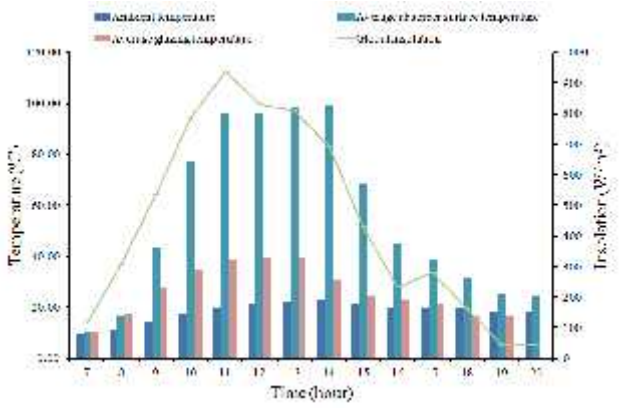

Fig. 7: Hourly solar radiation, stagnation temperature of the absorber surface, glazing surface temperature for prototype and ambient temperature

The day was sunny between 10 am and 2 pm. The maximum hourly absorber temperature reached 100^{o}C with maximum hourly solar radiation of 900 W/m^2. As there was no air flow the heat loss through the glazing was highest and the absorber and glazing temperature reached the highest temperature. The air flow from inlet to outlet helps to keep the stratified thermal layer from absorber surface to glazing. This thermal layer reduces heat loss through glazing surface due to convection and radiation. Glazing temperature reduces as the air flow rate increases.

3.3 Experimental results at low air flow

Table 2 shows a summary of the daily average performance of the closed loop glazed CTAH system with tertiary section at low air flow rate (0.03 kg/s/m^2). The experimental study at low air flow rate (0.03 kg/s/m^2) for closed loop glazed CTAH system with tertiary section were conducted between 25-27th July in 2011.

The results show that the average absorber temperature, outlet temperature and inlet temperature increased with solar radiation. The average solar radiation and ambient temperature varied between 364.7 W/m^2 and 891.9 W/m^2 and 18.8^{o}C and 25.5^{o}C on 25th July and 27th July respectively. The average thermal efficiency varied between 36.5% - 57.1% and effectiveness of the collector varied between 67.2% and 82%. It was found that the effectiveness was higher (82%) during low radiation level available (364.7 W/m^2) to the collector aperture.

However, effectiveness decreases to 67.2% with a higher radiation level (891.9 W/m^2). This reduction occurs due to higher thermal loss to the surrounding. The effectiveness of the closed CTAH was found to be higher compared to the open loop collector at low air flow (0.03 kg/s/m^2). The system performance is shown in Figure 8 at low air flow rate (0.03 kg/s/m^2) on the 27th July, 2011. The day was relatively sunny. The highest absorber temperature reached approximately 110^{o}C at midday when the sky was clear from morning to midday at average flow rate of 0.03 kg/s/m^2.

Table 2: Summary of daily performance at low air flow rate for closed loop glazed system for prototype 2 with tertiary section

Expt. Date	Avg. radiation (W/m^2)	Avg. absorber temp. (^{o}C)	Avg. outlet temp. (^{o}C)	Avg. inlet temp. (^{o}C)	Avg. ambient temp. (^{o}C)	Avg. efficiency (η)	Effectiveness (%)
25-Jul	364.7	32.7	30.2	22.5	18.8	36.5	82.0
26-Jul	571.8	52.8	45.4	26.8	21.5	54.9	76.4
27-Jul	891.9	77.3	60.3	30.1	25.5	57.1	67.2

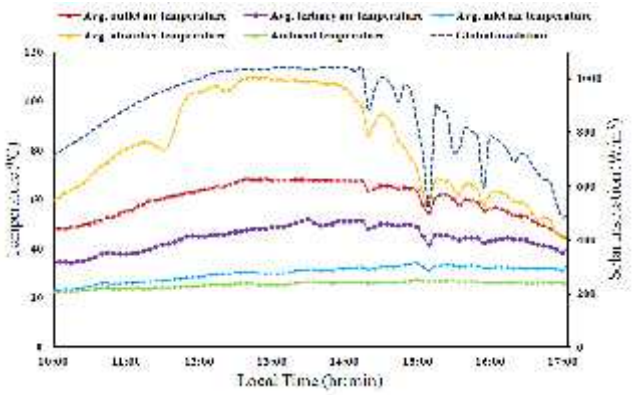

Fig. 8: Solar radiation, absorber surface temperature, outlet air temperature, inlet air temperature and ambient temperature at air flow rate 0.03 kg/s/m^2 for prototype

The highest outlet air temperature at the same flow rate in CTAH was 67.92^{o}C at an inlet temperature 31.09^{o}C and ambient temperature 26.08^{o}C.The outlet air temperature rise was 36.83^{o}C from inlet air temperature and the temperature rise was 41.84^{o}C from ambient air temperature. The hourly performance is shown in Figure 9. The average hourly insolation available on a relatively clear sky day from 10am to 5pm was 3.21 MJ/m^2. The average hourly useful energy from the collector was 1.82 MJ/m^2. The total available insolation for seven utilization hours was 22.47 MJ/m^2 and useful energy out of the collector was 12.9MJ/m^2 and average thermal efficiency was 57%.

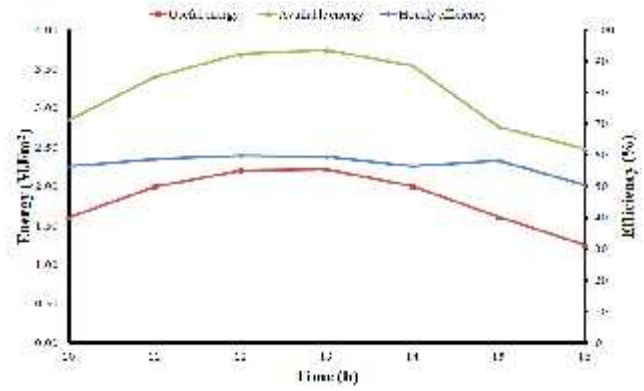

Fig. 9: Available hourly insolation, useful energy and thermal efficiency at air flow rate 0.03 kg/s/m^2 for prototype

4. Error Analysis

Solar radiation is strongly dependant on location and local weather so it is necessary to measure the available solar insolation for the test site. The incoming radiation was measured by a Kipp&ZonenCM6Bpyranometer with a maximum spatial intensity distribution of ±2%**.** The inlet air, outlet air, tertiary section air and absorber plate temperatures, were measured using type T (Cu-CuNi) PTFE insulated twist fine wire thermocouple sensor with accuracy of ±0.5^{o}C. All measurements were recorded at 1 minute intervals with a DL2e data logger. The data logger was connected directly to a computer where data was downloaded, read and extracted via a USB port. A small wind transmitter anemometer with accuracy of ±5% was used to measure wind speed. Inlet air flow rate was measured using an extech thermo anemometer with accuracy of ±5%. All thermocouples were labelled, inserted in a plug and connected to the data logger. The max. error was found below ±5% on output due to equipment and experimental accuracy.

5. Thermal Analysis

5.1 Energy delivered

The useful energy delivered by the solar collector was calculated using Equation 1[24-26].

$$Q_u = \dot{m}_{air} C_{pair} \left(T_{out} - T_{in} \right) \tag{1}$$

$$q_u = \frac{Q_u}{A_{apt}} \tag{2}$$

5.2 Collector Efficiency

The instantaneous efficiency η of a solar thermal collector can be defined as the ratio of the useful heat gain $\dot{Q}_u$ delivered per aperture area and the insulation I_G which is incident on the aperture.

$$\eta = \frac{\dot{Q}_u}{A_{apt} I_G} = \frac{\dot{q}_u}{I_G} \tag{3}$$

The useful heat is related to flow rate ($\dot{m}_{air}$), specific heat (C_{pair}) and inlet (T_{in}) and outlet (T_{out}) temperatures. The efficiency of the collector was calculated using Equation 5 [24]:

$$\eta_{collector} = \frac{\dot{m}_{air} C_{pair} \left(T_{out} - T_{in} \right)}{A_{apt} I_G} \tag{4}$$

6. Discussion

Figure 10 shows the air temperature rise of CTAH at different air flow rate (0.03 kg/s/m^2 to 0.09 kg/s/m^2).

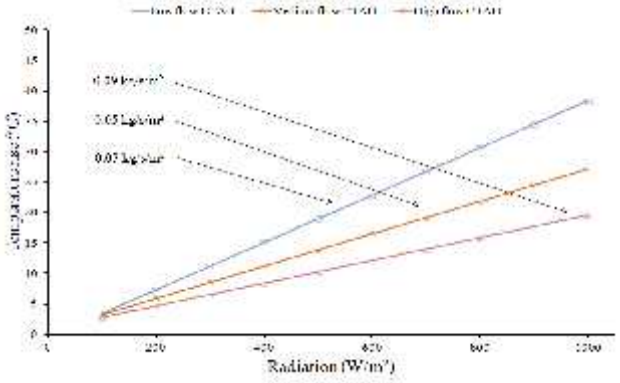

Fig. 10: Temperature rise of CTAH at various air flow rates and solar radiation levels

The lowest experimental operating flow rate (0.03 kg/s/m^2) resulted in the highest temperature rise of 38^{o}C at a radiation of 1000 W/m^2. The highest experimental operating flow rate (0.09 kg/s/m^2) on the other hand resulted in a temperature rise of 19.6^{o}C at a radiation of 1000 W/m^2.

The temperature rise was higher at all levels of radiation for an air flow rate 0.03 kg/s/m^2 compare to flow rate 0.09 kg/s/m^2. The air temperature rise for low and high flow rates was 19^{o}C and 10.3^{o}C at a solar radiation level of 500 W/m^2. The air temperature rise increases at higher radiation level and decreases at high air flow rate. However, the effect of radiation on temperature rise is more significant at higher level of solar radiation for both high and low air flow rates.

7. Conclusions

This research focused on the design and experimental performance analysis of a stationary new air heating system which is an integration of a Transpired Air-heating Collector (TAC) and an Asymmetric Compound Parabolic Concentrator (ACPC). Physical system design was carried out considering weight, cost and effectiveness. The main components of the system are an inverted perforated absorber, an ACPC concentrator, a parallel reflector section just below the inverted absorber and a glazing cover. An optical stationary concentrator was designed to concentrate solar radiation for 6-7 hours. Laser visualisation tests were carried out during the optical design process of the concentrator.

The basic optimisation factors considered in designing the CTAH system were to enhance the optical efficiency of the collector using a low concentration ratio concentrator; minimise the radiation and convection heat loss from absorber to ambient which can be achieved by using an inverted absorber facing downward; maximise convection heat transfer from absorber to inward airflow by using a perforated absorber and tertiary section to maintain a stable thermal layer in the concentrator cavity. minimise weight of the heating system by using a low weight perforated absorber; and minimise cost of the system by using unconventional low cost absorber material to avoid expensive selective coated metal absorber.Incorporation of carbon fibre as an absorber material reduces absorber weight which increases the acceptance possibility of the CTAH in building integration. For example: an aluminium absorber of Unglazed Transpired Collector (UTC) with identical thickness (0.26 mm) and perforation (4.1%) is 251% heavier than carbon fibre absorber of CTAH.

The instantaneous stagnation absorber temperature reached 135.9^{o}C. The lowest experimental operating flow rate (0.03 kg/s/m^2) resulted in the highest temperature rise of 38^{o}C at a radiation of 1000 W/m^2. The air temperature rise for low and high flow rates was 19^{o}C at a solar radiation level of 500 W/m^2.The highest experimental operating flow rate (0.09 kg/s/m^2) on the other hand resulted in a temperature rise of 19.6^{o}C at a radiation of 1000 W/m^2.The air temperature rise for high flow rates was 10.3^{o}C at a solar radiation level of 500 W/m^2. The air temperature rise increases at higher radiation level and decreases at high air flow rate.

Nomenclature

C_{pair}= specific heat capacity (kJ/kgK)

T_{out} = T_o=air temperature at collector outlet (^{o}C)

T_{in} = air temperature at collector inlet (^{o}C)

T_{amb}= ambient air temperature (^{o}C)

$\eta_{collector}$ = collector efficiency (dimensionless)

I_G = global solar irradiance (W/m^2)

Q_u = rate of useful energy delivered (W)

q_u = rate of useful energy per aperture area (W/m^2)

$\dot{m}_{air}$ = mass flow rate of air (kg/s)

References

1. Bhushan, B., & Singh, R. (2010). A review on methodology of artificial roughness used in duct of solar air heaters. *Energy, 35*(1), 202-212.
2. Chamoli, S., Chauhan, R., Thakur, N. S., & Saini, J. S. (2012). A review of the performance of double pass solar air heater. *Renewable and Sustainable Energy Reviews, 16*(1), 481-492.
3. Alta, D., Bilgili, E., Ertekin, C., & Yaldiz, O. (2010). Experimental investigation of three different solar air heaters: Energy and exergy analyses. *Applied Energy, 87*(10), 2953-2973.
4. Tanda, G. (2011). Performance of solar air heater ducts with different types of ribs on the absorber plate. *Energy, 36*(11), 6651-6660.
5. Gawlik, K., Christensen, C., & Kutscher, C. (2005). A numerical and experimental investigation of low-conductivity unglazed, transpired solar air heaters. *Journal of Solar Energy Engineering, Transactions of the ASME, 127*(1), 153-155.
6. Van Decker, G. W. E., Hollands, K. G. T., & Brunger, A. P. (2001). Heat-exchange relations for unglazed transpired solar collectors with circular holes on a square or triangular pitch. *Solar Energy, 71*(1), 33-45.
7. Mittal, M. K., & Varshney, L. (2006). Optimal thermohydraulic performance of a wire mesh packed solar air heater. *Solar Energy, 80*(9), 1112-1120.
8. Peng, D., Zhang, X., Dong, H., & Lv, K. (2010). Performance study of a novel solar air collector. *Applied Thermal Engineering, 30*(16), 2594-2601.

9. Rabl, A. (1976). Comparison of solar concentrators. *Solar Energy, 18*(2), 93-111.
10. Kienzlen, V., Gordon, J. M., & Kreider, J. F. (1988). Reverse flat plate collector: A stationary, nonevacuated, low-technology, medium-temperature solar collector. *Journal of Solar Energy Engineering, Transactions of the ASME, 110*(1), 23-30.
11. Kothdiwala, A. F., Norton, B., & Eames, P. C. (1995). The effect of variation of angle of inclination on the performance of low-concentration-ratio compound parabolic concentrating solar collectors. *Solar Energy, 55*(4), 301-309.
12. Eames, P. C., Norton, B., & Kothdiwala, A. F. (1996). The state of the art in modelling line-axis concentrating solar energy collectors. *Renewable Energy, 9*(1–4), 562-567.
13. Kothdiwala, A. F., Eames, P. C., & Norton, B. (1996). Optical performance of an asymmetric inverted absorber compound parabolic concentrating solar collector. *Renewable Energy, 9*(1–4), 576-579.
14. Rabl, A. (1985). *Active Solar Collectors and Their Applications*. New York: Oxford University Press.
15. Winston, R. (1974). Principles of solar concentrators of a novel design. *Solar Energy, 16*(2), 89-95.
16. Adsten, M. (2002). *Solar Thermal Collectors at High Latitudes: Design and Performance of Non-Tracking Concentrators.* (PhD), Uppsala University, Sweden.
17. Mallick, T. K. (2003). *Optics and heat transfer for asymmetric compound parabolic photovoltaic concentrators for building integrated photovoltaics.* (Ph.D), University of Ulster, Uk.
18. Nilsson, J. (2005). *Optical Design and Characterization of Solar Concentrators for Photovoltics.* (PhD), Lund University, Sweden.
19. Tchinda, R. (2008). Thermal behaviour of solar air heater with compound parabolic concentrator. *Energy Conversion and Management, 49*(4), 529-540.
20. Pramuang, S., & Exell, R. H. B. (2005). Transient test of a solar air heater with a compound parabolic concentrator. *Renewable Energy, 30*(5), 715-728.
21. Tiwari, G. N., & Suneja, S. (1997). *Solar thermal engineering systems*. UK: Narosa Publishing House.
22. Athienitis, A. K., Bambara, J., O'Neill, B., & Faille, J. (2011). A prototype photovoltaic/thermal system integrated with transpired collector. *Solar Energy, 85*(1), 139-153.
23. Odeh, N., Grassie, T., Henderson, D., & Muneer, T. (2006). Modelling of flow rate in a photovoltaic-driven roof slate-based solar ventilation air preheating system. *Energy Conversion and Management, 47*(7–8), 909-925.
24. Duffie, J. A., & Beckman, W. A. (2006). *Solar Engineering of Thermal Process* (3rd ed.). NY: J. W. & Sons.
25. Kalogirou, S. A. (2009). *Solar energy engineering, processes and systems*. USA: Elsevier.
26. Hastings, S. R., & Morck, O. (2000). *Solar air system: a design handbook*. UK: James and James Science.